

Thermosensitive Luminescent Lanthanide Complex with Two Photosensitized Ligands

Ayako Nakajima, Takayuki Nakanishi,* Yuichi Kitagawa,
Koji Fushimi, and Yasuchika Hasegawa

Faculty of Engineering, Hokkaido University,
Kita-13 jo, Nishi-8 chome, Kita-ku, Sapporo, Hokkaido 060-8626, Japan

(Received January 13, 2016; accepted May 16, 2016)

Keywords: thermosensor, lanthanide complex, energy transfer, luminescence

A novel thermosensitive luminescent lanthanide coordination compound was successfully synthesized. The coordination compound consists of Eu, Tb, and two photosensitized organic ligands [hexafluoroacetylacetone (hfa) and tris(*p*-carboxyphenyl) phosphine oxide (TPO)]. The Eu/Tb mixed coordination compound shows different luminescent colors depending on the temperature (green luminescence at 300 K and yellow luminescence at 450 K). In this study, emission spectra were measured at 300, 350, 400, and 400 K, and the ratio of (Eu/Tb) luminescence intensity at each temperature was estimated. The temperature-dependent luminescence is caused by the two differentially photosensitized organic ligands, hfa and TPO. These results may lead to the development of novel thermosensing devices using lanthanide luminescence.

1. Introduction

Accurate measurements of the physical parameters of material surfaces are important in the area of environmental engineering. Optoelectronic devices have been used as both thermosensors and pressure sensors.⁽¹⁾ In this study, we focused on a two-dimensional thermosensor based on a luminescent lanthanide complex.

A lanthanide complex is a useful candidate for thermo- and pressure-sensitive dyes. The lanthanide complexes with characteristic narrow emission bands based on $4f-4f$ transitions have been regarded as attractive luminescent materials for use in lasers,^(2,3) organic LEDs⁽⁴⁻⁷⁾ and bio-imaging⁽⁸⁻¹⁰⁾ applications. Efficient energy transfer from organic ligands to lanthanide ions, i.e., photosensitized energy transfer, is required to produce strong luminescence, because the $4f-4f$ transitions are Laporte forbidden, and as such have small absorption coefficients ($\epsilon < 10 \text{ M}^{-1} \text{ cm}^{-1}$). A strong luminescent lanthanide complex can function as a sensor. We also have reported thermosensing materials based on lanthanide coordination polymers.^(11,12)

Here, we report on a coordination compound composed of lanthanide ions and two different ligands. Eu and Tb mixed coordination compounds using tris(*p*-carboxyphenyl) phosphine oxide (TPO) and hexafluoroacetylacetonate (hfa: photosensitized ligand) ligands were prepared as thermosensing materials. The combination of red luminescent Eu ions and green luminescent Tb ions in the coordination compound provides thermosensing abilities between 300–450 K. The Eu/

*Corresponding author: e-mail: nakanishi@eng.hokudai.ac.jp

Tb coordination compound is expected to open up a new field of thermosensing materials. In this study, we focus on a Eu/Tb coordination compound with hfa and TPO ligands as a photosensitizer. The thermosensing property of a Eu/Tb coordination compound has been demonstrated for the first time.

2. Materials and Methods

2.1 Materials

Europium acetate tetrahydrate (99.9%), terbium acetate tetrahydrate (99.9%), and tri-*p*-tolylphosphine were purchased from Wako Pure Chemical Industries Ltd. Hexafluoroacetylacetone was obtained from Tokyo Kasei Organic Chemicals Co., Inc. Dimethyl sulfoxide-*d*₆ (D, 99.9%) was obtained from Kanto Chemical Co., Inc. All other chemicals and solvents were reagent grade and were used without further purification.

2.2 Preparation of TPO

TPO was synthesized by the oxidation of tri-*p*-tolylphosphine (2.0 g, 3.1 mmol) with potassium permanganate (20.0 g, 63.3 mmol) in pyridine and H₂O.⁽¹³⁾ Yield: 34%; ¹H nuclear magnetic resonance (NMR) (400 MHz, DMSO-*d*₆, 298 K): δ 8.12–8.08 (*dd*, 6H), 7.88–7.75 (*dd*, 6H) ppm; IR (ATR): 1692, 1395, 1246, 1162, 1102, 1016 cm⁻¹; Elemental analysis calcd (%) for [C₂₁H₁₅O₇P + H₂O]: C 58.89, H 4.00; found: C 58.67, H 4.08.

2.3 Preparation of Eu(hfa)₃(H₂O)₂ and Tb(hfa)₃(H₂O)₂

Europium acetate tetrahydrate (5.0 g, 13.6 mmol) was dissolved in distilled water (20 mL). A solution of hexafluoroacetylacetone (7.0 g, 33.6 mmol) was added dropwise to the solution. The reaction mixture produced a precipitate of white yellow powder after stirring for 3 h at room temperature. The reaction mixture was filtered, and the resulting powder was used without further purification for the next step. Yield: 95%; IR (KBr): 1650, 1258–1145 cm⁻¹; Elemental analysis calcd (%) for C₁₅H₇EuF₁₈O₈: C 22.27, H 0.87; found: C 22.12, H 1.01.⁽¹⁴⁾ Terbium acetate tetrahydrate (5.0 g, 12.3 mmol) was dissolved in distilled water (20 mL). A solution of hexafluoroacetylacetone (7.0 g, 33.6 mmol) was added dropwise to the solution. The reaction mixture produced a precipitate of white yellow powder after stirring for 3 h at room temperature. The reaction mixture was filtered, and the resulting powder was used without further purification for the next step. Yield: 70%; IR(KBr): 1650, 1255–1141 cm⁻¹; Elemental analysis calcd (%) for [C₁₅H₇F₁₈O₈Tb + H₂O]: C 21.60, H 1.09; found: C 21.47, H 1.34.⁽¹⁵⁾

2.4 Preparation of Eu/Tb(hfa)_x(TPO)_y

TPO (0.08 g, 0.2 mmol) was dissolved in methanol (2 ml) at 323 K and Eu(hfa)₃(H₂O)₂ (0.16 g, 0.19 mmol) and Tb(hfa)₃(H₂O)₂ (0.08 g, 0.10 mmol) in methanol (2 ml) were added. The precipitates were filtered, washed with methanol several times, and dried *in vacuo*. Inductively coupled plasma atomic emission spectrometry (ICP-AES): Eu:Tb = 1.0:18.4.

2.5 Preparation of $\text{Gd}(\text{hfa})_x(\text{TPO})_y$

TPO (0.12 g, 0.3 mmol) was dissolved in methanol (2 ml) at 323 K and $\text{Gd}(\text{hfa})_3(\text{H}_2\text{O})_2$ (0.24 g, 0.3 mmol) in methanol (2 ml) was added. The precipitates were filtered, washed with methanol several times, and dried *in vacuo*.

2.6 Apparatus

^1H NMR (400 MHz) spectra were recorded on a JEOL ECS400. Chemical shifts were reported in δ ppm, referenced to an internal tetramethylsilane (TMS) standard for ^1H NMR spectroscopy. Elemental analyses were performed on a J-Science Lab Micro Corder JM 10 and an Exeter Analytical CE440. The ratio of F to Eu was measured using an energy dispersive X-ray fluorescence spectrometer EDX-8000 with the reference material $\text{Eu}(\text{hfa})_3(\text{TPPO})_2$,⁽¹¹⁾ and the Eu/Tb ratio was measured using ICP-AES Shimadzu ICPE-9000. X-ray diffraction (XRD) patterns were characterized using a Rigaku SmartLab X-ray diffractometer with Cu K_α radiation, a D/teX Ultra detector, and a temperature control unit (Anton Paar, TCU-110).

Emission and excitation spectra of $\text{Eu/Tb}(\text{hfa})_x(\text{TPO})_y$ at room temperature were recorded on a HORIBA Fluorolog-3 spectrofluorometer and corrected for the response of the detector system. Emission spectra of $\text{Eu/Tb}(\text{hfa})_x(\text{TPO})_y$ in the 300–450 K range were recorded on a JASCO F-6300-H spectrometer under temperature control using a cryostat (Thermal Block Company, SA-SB245T) and a temperature controller (Scientific Instruments, Model 9700).

3. Results and Discussion

$\text{Eu/Tb}(\text{hfa})_x(\text{TPO})_y$ was synthesized by the complexation of Eu(III) and Tb(III) ions with hfa and TPO ligands. Carboxy phosphine oxide (TPO), $\text{Eu}(\text{hfa})_3(\text{H}_2\text{O})_2$, and $\text{Tb}(\text{hfa})_3(\text{H}_2\text{O})_2$ (TPO:Eu:Tb = 21:1:20, molar ratio) were added in methanol and refluxed at 333 K for 10 h (Fig. 1). The details of structural features [$\text{Eu}(\text{hfa})_x(\text{TPO})_y$] including single-crystal structure are described in our previous paper.⁽¹⁶⁾ The x and y in $\text{Eu}(\text{hfa})_x(\text{TPO})_y$ were determined to be $0 < x < 1$ and $0 < y < 3$ using EDX data. The Eu:Tb ratio of $\text{Eu/Tb}(\text{hfa})_x(\text{TPO})_y$ using ICP-AES data was determined to be 1.0:18.4.

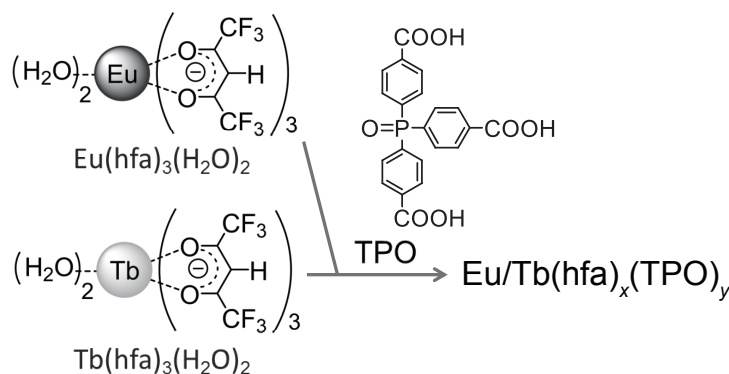


Fig. 1. Molecular structures of $\text{Eu}(\text{hfa})_3(\text{H}_2\text{O})_2$ and $\text{Tb}(\text{hfa})_3(\text{H}_2\text{O})_2$, and the synthesis of $\text{Eu/Tb}(\text{hfa})_x(\text{TPO})_y$.

The crystallinity and the crystal phase⁽¹⁶⁾ of $\text{Eu/Tb(hfa)}_x(\text{TPO})_y$ were characterized by XRD measurements. Diffraction peaks in XRD measurement at 11.37, 14.66, 18.60, 19.53, 23.54, 28.20, 30.20, and 31.78° were observed, and the Eu/Tb compound possessed high crystallinity based on an ordered lattice arrangement. The thermal properties of $\text{Eu/Tb(hfa)}_x(\text{TPO})_y$ were the same as that of $\text{Eu(hfa)}_x(\text{TPO})_y$, which was reported in our recent paper,⁽¹⁶⁾ and the decomposition temperature was 723K. Therefore, we successfully prepared a crystalline Eu/Tb compound with organic ligands.

Emission spectra of $\text{Eu/Tb(hfa)}_x(\text{TPO})_y$ were measured under nitrogen gas atmosphere [Fig. 2(a)]. Color pictures at 300 and 400 K are shown in Fig. 2(b). The emission bands observed at 490, 544, 583, 620, 644, and 668 nm are attributed to the $4f-4f$ transitions of Tb(III) ($^5\text{D}_4 \rightarrow ^7\text{F}_j$; $J = 6-1$), and these at 590, 613, 652, and 699 nm are attributed to the $4f-4f$ transitions of Eu(III) ($^5\text{D}_0 \rightarrow ^7\text{F}_j$; $J = 1-4$). The luminescence intensity of Tb decreased monotonically with increasing temperature from 300 to 450 K. On the other hand, the luminescence intensity of Eu increased between 300 and 350 K, and then it decreased from 350 to 450 K. Figure 2(c) shows the temperature dependence of the (Eu/Tb) luminescence intensity ratio. This result indicates that the compound possesses effective thermosensing properties over a narrow temperature range, 300–350 K.

$\text{Eu/Tb(hfa)}_x(\text{TPO})_y$ includes two organic ligands with different photosensitization efficiencies. When $\text{Eu/Tb(hfa)}_x(\text{TPO})_y$ is irradiated with UV light ($\lambda < 400$ nm), the ligands are in an excited singlet state. Then, the ligands change to an excited triplet state via intersystem crossing. Energy transfer from the triplet state to the emitting level of the lanthanide ions is promoted after the formation of the triplet state of the ligands. The triplet levels of hfa and TPO ligands affect the temperature dependence of the luminescence. The emitting level of Tb ($^5\text{D}_4$; 20534 cm^{-1})⁽¹⁷⁾ is close to the triplet level of the hfa ligand (22000 cm^{-1}).⁽¹¹⁾ It is well known that thermal quenching between Tb and hfa occurs easily. In contrast, the combination of Eu and hfa shows little thermal quenching, because of the wide gap ($\Delta 4773 \text{ cm}^{-1}$) between the emitting level of Eu ($^5\text{D}_0$; 17227

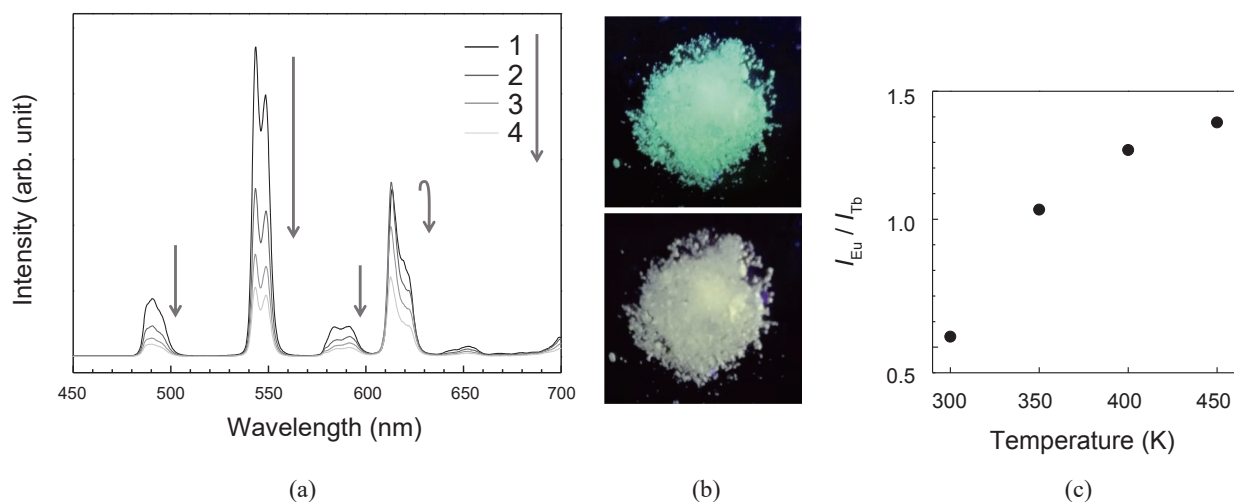


Fig. 2. (Color online) (a) Emission spectra of $\text{Eu/Tb(hfa)}_x(\text{TPO})_y$ in the solid state measured at 300 K (line 1), 350 K (line 2), 400 K (line 3), and 450 K (line 4), excited at 355 nm. (b) Color pictures at 300 K (upper) and 400 K (lower), excited at 365 nm. (c) Temperature dependence of (Eu/Tb) luminescence intensity ratio, $I_{\text{Eu}} / I_{\text{Tb}}$, estimated from emission spectra at 613 nm (Eu: $^5\text{D}_0 \rightarrow ^7\text{F}_2$) and 543 nm (Tb: $^5\text{D}_4 \rightarrow ^7\text{F}_5$).

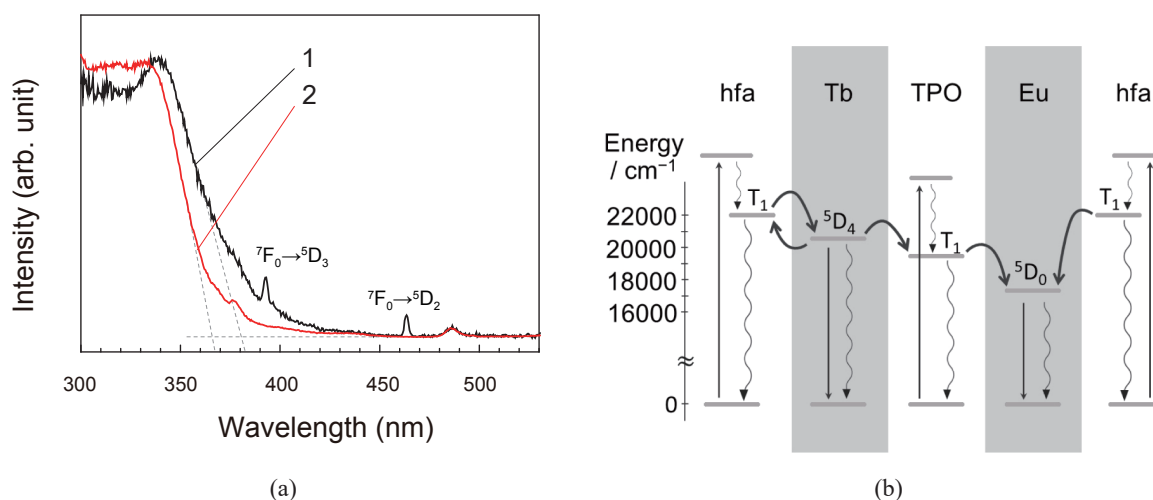


Fig. 3. (Color online) (a) Excitation spectra of $\text{Eu/Tb(hfa)}_x(\text{TPO})_y$ in the solid state detected at 610 nm (Eu: ${}^5\text{D}_0 \rightarrow {}^7\text{F}_2$; line 1) and 545 nm (Tb: ${}^5\text{D}_4 \rightarrow {}^7\text{F}_5$; line 2). Two cross marks of dashed lines indicate the photosensitized absorption rising edges from organic ligands. (b) Postulated energy diagram of $\text{Eu/Tb(hfa)}_x(\text{TPO})_y$.

cm^{-1})⁽¹⁸⁾ and the triplet level of the hfa ligand.^(11,12) In our experiment on the temperature dependence of the luminescence intensity, we observed a significant increase in Eu-emission intensity between 300 and 350 K. Therefore, we considered the photosensitized emission mechanism based on hfa and TPO ligands.

The excitation spectra of $\text{Eu/Tb(hfa)}_x(\text{TPO})_y$ monitored at 610 nm (Eu: ${}^5\text{D}_0 \rightarrow {}^7\text{F}_2$) and 545 nm (Tb: ${}^5\text{D}_4 \rightarrow {}^7\text{F}_5$) are shown in Fig. 3(a). The estimated absorption edge of the excitation spectrum is longer at 610 nm than at 545 nm. The longer absorption edge at 610 nm is caused by energy transfer from TPO to Eu. Energy levels of the triplet state of a ligand in general can be estimated using a Gd complex at low temperature.⁽¹⁹⁾ By phosphorescence measurements ($\lambda_{\text{ex}} = 355 \text{ nm}$) using $\text{Gd(hfa)}_x(\text{TPO})_y$, the triplet state of TPO is calculated to be 19500 cm^{-1} . The triplet level is lower than the emitting level of Tb (${}^5\text{D}_4$: 20534 cm^{-1}). Figure 3(b) shows an energy diagram of $\text{Eu/Tb(hfa)}_x(\text{TPO})_y$. The temperature-dependent luminescence might be associated with photosensitized TPO ligands. The Eu/Tb coordination compound with two types of photosensitized ligand leads to the temperature dependence of luminescence. The Eu/Tb compound is expected to be a candidate for a thermosensitive dye.

4. Conclusions

A novel thermosensing Eu/Tb mixed compound was successfully synthesized. This compound showed thermosensing in the range of 300–350 K. In the future, $\text{Eu/Tb(hfa)}_x(\text{TPO})_y$ is expected to be a promising candidate for a thermosensitive dye, which could be used for temperature distribution measurements on material surfaces.

Acknowledgements

We thank Shimadzu Corporation, Mr. Nishino, and Akira Suzuki of Frontier Chemistry Center “Laboratories for Future Creation” Project. This work was supported by a Grant-in-Aid for Scientific Research on Innovative Areas of “New Polymeric Materials Based on Element Blocks (no. 2401)” (no. 24102012) from the Ministry of Education, Culture, Sports, Science and Technology (MEXT), Japan. This work was partially supported by the Cooperative Research Project of the Research Institute of Electronics, Shizuoka University.

References

- 1 M. Kameda, N. Tezuka, T. Hangai, K. Asai, K. Nakakita, and Y. Amao: Proceedings of MOSAIC International Workshop, November 10–11, 2003, Tokyo, Japan.
- 2 P. K. Shahi, A. K. Singh, S. B. Rai, and B. Ullrich: *Sens. Actuators, A* **222** (2015) 255.
- 3 P. K. Shahi, A. K. Singh, S. K. Singh, S. B. Rai, and B. Ullrich: *ACS Appl. Mater. Interfaces* **7** (2015) 18231.
- 4 J. Wang, C. Han, G. Xie, Y. Wei, Q. Xue, P. Yan, and H. Xu: *Chem. Eur. J.* **20** (2014) 11137.
- 5 Z. Ahmed and K. Iftikhar: *RSC Adv.* **4** (2014) 63696.
- 6 Y. Cui, B. Chen, and G. Qian: *Coord. Chem. Rev.* **273–274** (2014) 76.
- 7 H. Xu, J. Wang, Y. Wei, G. Xie, Q. Xue, Z. Deng, and W. Huang: *J. Mater. Chem., C* **3** (2015) 1893.
- 8 J. R. Diniz, J. R. Correa, D. de A. Moreira, R. S. Fontenele, A. L. de Oliveira, P. V. Abdelnur, J. D. Dutra, R. O. Freire, M. O. Rodrigues, and B. A. D. Neto: *Inorg. Chem.* **52** (2013) 10199.
- 9 V. Placide, A. T. Bui, A. Grichine, A. Duperray, D. Pitrat, C. Andraud, and O. Maury: *Dalton Trans.* **44** (2015) 4918.
- 10 Z. Liang, C.-F. Chan, Y. Liu, W.-T. Wong, C.-S. Lee, G.-L. Law, and K.-L. Wong: *RSC Adv.* **5** (2015) 13347.
- 11 K. Miyata, Y. Konno, T. Nakanishi, A. Kobayashi, M. Kato, K. Fushimi, and Y. Hasegawa: *Angew. Chem. Int. Ed.* **52** (2013) 6413.
- 12 Y. Hirai, T. Nakanishi, K. Miyata, K. Fushimi, and Y. Hasegawa: *Mater. Lett.* **130** (2014) 91.
- 13 J. Václavík, M. Servalli, C. Lothschütz, J. Szlachetko, M. Ranocchiaro, and J. A. van Bokhoven: *ChemCatChem* **5** (2013) 692.
- 14 Y. Hasegawa, T. Ohkubo, T. Nakanishi, A. Kobayashi, M. Kato, T. Seki, H. Ito, and K. Fushimi: *Eur. J. Inorg. Chem.* **2013** (2013) 5911.
- 15 S. Katagiri, Y. Tsukahara, Y. Hasegawa, and Y. Wada: *Bull. Chem. Soc. Jpn.* **80** (2007) 1492.
- 16 A. Nakajima, T. Nakanishi, Y. Kitagawa, T. Seki, H. Ito, K. Fushimi, and Y. Hasegawa: *Sci. Rep.* **6** (2016) 24458.
- 17 S. Omagari, T. Nakanishi, T. Seki, Y. Kitagawa, Y. Takahata, K. Fushimi, H. Ito, and Y. Hasegawa: *J. Phys. Chem., A* **119** (2015) 1943.
- 18 K. Binnemans: *Coord. Chem. Rev.* **295** (2015) 1.
- 19 M. Latva, H. Takalo, V.-M. Mukkala, C. Matachescu, J. C. Rodríguez-Ubis, and J. Kankare: *J. Lumin.* **75** (1997) 149.